Astron. Astrophys. 316, 499–505 (1996)

ASTRONOMY
AND
ASTROPHYSICS

Joint Ulysses and WIND observations of a particle event in April 1995

A. Buttighoffer[1], M. Pick[1], A. Raviart[2], S. Hoang[3], R.P. Lin[4], G.M. Simnett[5], L.J. Lanzerotti[6], and V. Bothmer[7]

[1] DASOP, URA 2080, Observatoire de Meudon, F-92195 Meudon, France
[2] CEA-Saclay, DSM, DAPNIA, Service d'Astrophysique, F-91191, France
[3] DESPA, URA 246, Observatoire de Meudon, F-92195 Meudon, France
[4] Department of Physics and Space Sciences Laboratory, University of California, Berkeley, CA 94720, USA
[5] University of Birmingham, Birmingham, UK
[6] AT&T Bell Laboratories, Murray Hill, NJ 07974, USA
[7] Space Science Department of ESA, ESTEC, 2200 AG Noordwijk, The Netherlands

Received 16 February 1996 / Accepted 24 July 1996

Abstract. In this paper we analyze a solar particle event that was measured at two locations in the heliosphere. Ulysses was at 40° north heliolatitude and 130° west in heliolongitude from Earth while WIND was near Earth at 1 AU in the ecliptic plane. To establish the origin of the particle events, solar coronal activity is investigated. Direct observational evidence of the association between long–duration electron acceleration and a solar radio noise storm is shown. We also establish that the interplanetary type III burst studied here is produced by successive electron injections from distinct coronal locations. Two particle increases are observed during the event. For the first one, the particles are shown to be from coronal origin; for the second one, which is associated with a Forbush decrease, the particles are primarily shock accelerated. The differences in particle intensities observed at WIND and Ulysses are explained by the nature of the particle propagation to the spacecraft locations.

Key words: interplanetary medium – Sun: particle emission – Sun: radio radiation – Sun: corona

1. Introduction

The particle event discussed here was observed in late April 95 by the HI-SCALE (Lanzerotti et al., 1992) and COSPIN (Simpson et al., 1992) instruments aboard Ulysses and the 3D Plasma and Energetic Particle (3DP) experiment aboard WIND (Lin et al., 1995). At this time Ulysses was located at 40° north heliolatitude and 130° west heliolongitude, at a distance of 1.5 AU from the Sun. Ulysses was making its first south–to–north heliolatitude pass. This event was the last major event observed by HI-SCALE before the north solar pass.

Send offprint requests to: A. Buttighoffer

At Ulysses, the event appears clearly on hourly–averaged data as shown in Fig. 1 (upper panel), as an electron event with a rapid onset and a slow decay. The maximum phase of this event consists of two successive peaks which occur on April 22 and April 25. The first electron peak was not accompanied by ions within the HI-SCALE energy ranges, but is discernible above 5.4 MeV by the COSPIN/KET telescope (bottom panel in the figure). The second peak has a ion–counterpart, both in the HI-SCALE and COSPIN energy ranges (center two panels). A Forbush–like decrease is observed at Ulysses in the 320–2200 MeV proton COSPIN channel during the second particle increase (see Fig. 3). The 3DP instrument aboard WIND observed two electron peaks on April 22 and April 26 which both had a proton counterpart (two lower panels of Fig. 3); they were superimposed on a gradual rise and fall in the 1 AU electron intensity.

The only active region on the visible hemisphere of the Sun during this time was #7863, which produced Hα flares on April 19, 21 and 22 prior to its rotation behind the west limb (Solar Geophysical Data, May–July 1995). These flares were associated with X–Ray bursts as measured by the Earth–orbiting geosphere satellite GOES 8.

In this paper we analyze the time dependence of the interplanetary particles measured by the Ulysses and WIND spacecraft during the April 20 to May 1 period. During this period the two spacecraft are at different locations in the heliosphere, separated by 0.42 AU in radial distance to the Sun, 40° in heliolatitude and 130° in longitude. After briefly describing the instruments used in this study, we present a detailed analysis of the particle behavior and local plasma parameters at both spacecraft. We then examine the coronal activity as revealed by optical, radio and X–Ray observations made from the two different locations of Ulysses and WIND. Finally we discuss the

Table 1. Parker Spiral model for Ulysses and WIND for April 22, 1995.

Spacecraft	Solar wind km/s	lat. °	Heliographic long. °	range AU	Foot point pos. °	Plasma conv. time h	Spiral length AU
Ulysses	750	37N	133W	1.42	37N–178W	80	1.5
WIND (Earth)	310	0N	0W	1	0N–77W	134	1.2

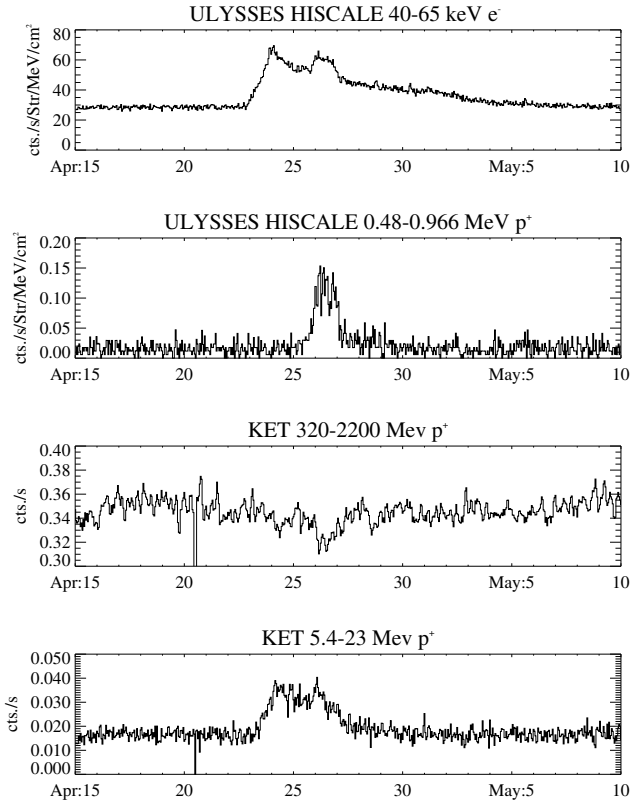

Fig. 1. Hourly averaged data from the Ulysses HI-SCALE and KET instruments are plotted here versus time from April 15 to May 05, 1995. From top to bottom the four panels display HI-SCALE 40–65 keV electron fluxes; HI-SCALE 0.480–0.966 keV proton fluxes; KET 320–2200 Mev protons counting rates and KET 5.4–23 MeV proton counting rates.

interpretation of the particle observations made by Ulysses and WIND during this period.

2. Instrumentation

The Heliosphere Instrument for Spectra, Composition, and Anisotropy at low energies (HI-SCALE; Lanzerotti et al., 1992) aboard Ulysses consists of three solid–state particle telescopes, each containing a pair of 200μm Si detectors. The two "rates" telescopes each have two oppositely–directed apertures which are at angles of 30/150° (M for magnetic and F for foil detectors) and 60/150° (M′& F′) to the spin axis. The LEFS (Low Energy Foil Spectrometer) apertures have a thin foil in front of the detector to remove low–energy ions, thus allowing the detector to respond to ∼40–280 keV electrons. In the LEMS (low Energy Magnetic Spectrometer) apertures, electrons are deflected by a magnet away from the detectors. In the LEMS30 aperture (at 30° to the spin axis), the electrons are directed into the back (B) detector of the third (Composition Aperture, CA) telescope. The two telescope heads are about 15 cm apart on one corner of the spacecraft. In each detector pair, the rear detector is used as anticoincidence guard. Each LEMS rate is divided into 8 energy channels and each LEFS into 7; a "single" rate is also recorded for each detector. Almost complete 4π sr. coverage is obtained once per spacecraft spin (5 rpm). Solar X–Rays may be detected in two sectors of LEMS30 in the low energy channels.

The COsmic ray Solar Particle INvestigation (COSPIN; Simpson et al., 1992) consists of a set of 4 different instruments and is designed to make composition and anisotropy measurements of electrons from 2.5 to 6000 MeV and ions from 0.5 to 600 MeV/nucleon. In this article we have used data from two of those instruments: the Kiel Electron Telescope (KET) which measures electrons, protons and helium nuclei from a few MeV to a few GeV; we also had information from the Low Energy Telescope (LET) measuring the spectra and composition of ions between 1 and 75 MeV and electrons in the 0.3–1 MeV ranges.

The 3DP instrument aboard WIND is described by Lin et al. (1995). This instrument is designed to obtain the full 3–D distribution of suprathermal electrons and ions from the solar wind to ∼ 300 keV. Electrons from 20 keV to ∼1 MeV and ions up to ∼1 MeV are detected by semi–conductor telescopes with a full 4π sr. coverage as fast as a spin period (3s). Electrons and ions from ∼3 eV to 30 keV are detected by electrostatic analyzers with a 4π sr. coverage, also as fast as a spin period (3s). Earth bow shock–related events have been eliminated from the 3DP data, leaving only the solar and interplanetary events.

The radio emissions reported in this paper were made by the Radio Astronomy Receiver of the Ulysses Unified Radio and Plasma (URAP) experiment (Stone et al., 1992). This instrument operates over two bands: a high–frequency band with 12 logarithmically spaced frequencies between 52 and 940 kHz and a low–frequency band consisting of 64 frequencies linearly spaced between 1.25 and 48.5 kHz. Some solar type III bursts observed here have been followed from 1 MHz down to some tens of kHz thanks to this instrument. The observation of the

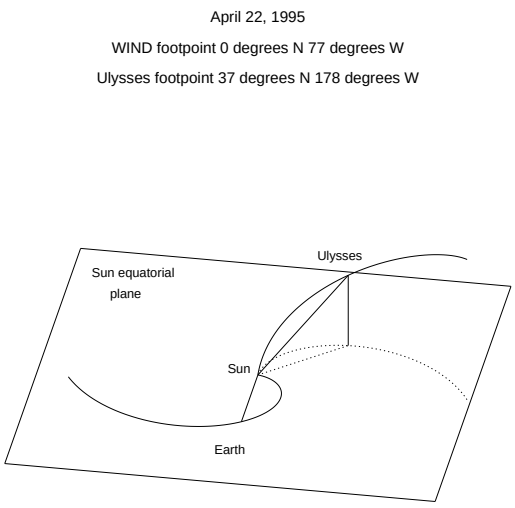

Fig. 2. Parker spiral geometry for April 22, 1995 for Ulysses spacecraft and WIND/Earth connections. The Ulysses spacecraft spiral has been computed for a solar wind speed of 750 km/s. WIND/Earth spiral has been computed for a solar wind speed of 310 km/s and is represented in dotted line. See Table 1 for details. The projections of the corresponding spirals onto the ecliptic are represented at the bottom of the figure.

thermal plasma noise around the plasma frequency also gives an indication of the local plasma conditions and in particular when solar wind disturbances are convected past the spacecraft.

The temporal and spatial evolution of solar radio activity as seen from Earth is studied in detail by the Nançay Radioheliograph (after NRH; The radioheliograph group, 1993). The NRH is a multi–array interferometer operating with 0.1 s time resolution at 5 frequencies between 150 and 450 MHz, effectively sounding five different altitudes in the solar corona.

3. Observations

3.1. An overview

The respective positions of Ulysses, WIND and Earth are represented in Fig. 2 with the theoretical Parker spirals connecting them to the Sun. Calculations were made with a solar wind speed of 750 km/s for Ulysses (as measured by the solar wind instrument on the spacecraft) and 310 km/s for WIND/Earth (from IMP8 measurements printed in Solar Geophysical Data) and are summarized in Table 1. Ulysses is located at a longitude of about 130° away from the Earth/Sun line and at 40° north of the ecliptic plane. This positions the supposed Ulysses' Parker spiral footpoint on the invisible side of the Sun as seen from Earth (180° for the observed solar wind speed of about 750 km/s). The whole geometry is sketched in Fig. 2.

A careful timing analysis of Ulysses south–to–north pass (see Roelof et al., this issue) shows that the event observed at Ulysses can not be CIR–associated. Moreover, as noted in this paper, the asymmetric shape of the HI-SCALE electron flux enhancement (see Fig. 1) is not consistent with those associated to CIRs and is rather in favor with a solar origin event.

3.2. Particle events and plasma

As discussed in the Introduction, the HI-SCALE electron and ion fluxes as measured during this period have a distinct temporal evolution (see the two top panels of Fig. 1). The upper panel in Fig. 1 shows the 40-65 keV electron rate from the LEFS150 telescope. For this energy channel, the intensity starts to increase above the pre–event level around April 22, 21:00 UT and around 19:00 UT in the 60-107 keV channel (not shown in Fig. 1); after the maximum, a slow exponential decrease occurs until the fluxes reach their pre–event level on May 06. This decreasing phase is interrupted from April 25, 24:00 UT, until April 27, 00:00 UT, by a superimposed second event. During the beginning of this second event, a weak electron anisotropy is discernable as LEFS60 fluxes seem to increase slightly before LEMS150 fluxes (i.e. the first electrons to arrive are from the solar direction). The most important difference between those 2 events is the lack of any ion counterpart at low energies during the first increase as will be shown below.

An ion counterpart to the first electron event is observed by the COSPIN/HET, KET and LET experiment above 1.2 MeV. The time history of the 5.4–23 MeV KET proton channel is shown in more detail than in Fig. 1 in the second from the top panel of Fig. 3. The onset times of the three COSPIN channels have been estimated to be around April 23, 00–1:00 UT for HET (14–19 MeV); 3–4:00 UT for KET (5.4–23 MeV) and 18–19:00 UT for LET (1.2–3 MeV). No ion–counterpart is seen below 1 MeV as measured by the HI-SCALE channels (see third from top–left and right panels of Fig. 3). On the contrary, the second electron event has a counterpart detected in the HI-SCALE 0.5–1 MeV proton channels, which abruptly increase from April 25, around 12:00 UT and persists to about April 27, 0:00 UT. This event is also seen as a very sharp increase in the MeV proton range by COSPIN/LET and above 5 MeV by COSPIN/KET.

This second event appears to occur around April 25, 12:00 UT, with no time dispersion in the various electron and proton channels, as shown in Fig. 1. The high energy COSPIN protons (320–2200 MeV of KET) exhibit an associated Forbush–like flux decrease at about the time of the second event (top panels in Fig. 3). On April 27, 0:00 UT, the COSPIN and HI-SCALE proton channels abruptly decrease with the HI-SCALE electron fluxes, which then follow the exponential decrease that began after the first peak of April 24. None of the ion flux increases in the HI-SCALE data is associated with strong anisotropy.

The $Z>2$ composition of the interplanetary particles at Ulysses was investigated during the event using measurements made by the HI-SCALE CA telescope. The fluxes of all ions were found to be very low. During the interval of the second particle enhancement, two Ne ions (0.8–5 MeV/nucl) were detected. While this is a very small number statistically, it can be considered significant in that for more than ten days prior, and

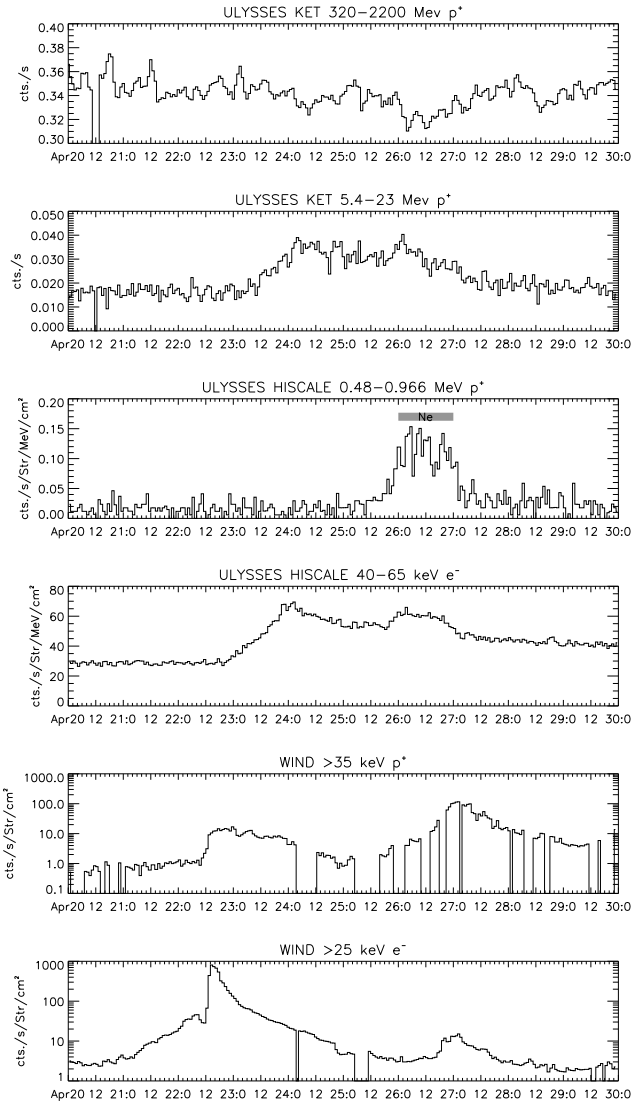

Fig. 3. This figure presents the flux or counting rate histories of various channels aboard Ulysses (four top panels) and WIND (two last panels) spacecraft. From top to bottom, hourly–averaged rates of COSPIN/KET 320–2200 MeV protons; 5.4–23 MeV protons; HI-SCALE fluxes of 0.48–0.966 MeV protons; 40–65 keV electrons; WIND/3DP fluxes of >35 keV protons; >25 keV electrons. Earth bow shock–related events have been excised from WIND data (the two last panels) which are presented here in a logarithmic scale. The thick bar on the HI-SCALE proton panel represents the time interval during which Ne ions were detected.

more than ten days after, the interplanetary electron enhancement at Ulysses, there was no detection of any Ne ion. It was not possible to conclude that there were any statistical changes in the interplanetary O ions above the fluxes that were observed throughout the more than twenty days around the overall event. The observed fluxes of O are essentially low energy anomalous cosmic ray oxygen ions.

During this period no major structures are identified in the solar wind plasma parameters at Ulysses. There are nevertheless two noticeable plasma features at Ulysses. On April 23, an augmentation of the plasma frequency is observed by RAR from 14:40 UT to 19:50 UT. This observation is not accompanied by any signature in the solar wind SWOOPS instrument (Bame et al., 1992) data. However, around 12:00 UT on this day, a sharp decrease is observed in the plasma temperature; this decrease is associated with discontinuities in the solar wind speed. Another period of interest is around April 27, when the solar wind velocity decreases and the total magnetic field shows an abrupt increase.

Table 2. Low frequency type III bursts onsets (at 1 MHz) and corresponding X–Ray bursts (from HI-SCALE pseudo X–Ray channels).

Date	TIII	X–Ray
April 20		
April 21		12h
April 22	11h50/12h30	11h48
April 25	04h50	05h
April 26	01h15-10h40	– -10h36
April 27	03h20/03h40	–
April 28	16h40/17h05	–

Particle observations near the Earth from WIND reveal a gradual rise in the flux of electrons >25 keV beginning around 06:00 UT on April 21, with no corresponding increase in >35 keV ions (lower two panels in Fig. 3). The rise reaches a flux of ~ 40 $(\mathrm{cm}^2.\mathrm{s.sr})^{-1}$ just prior to the onset of an intense solar flare energetic particle event beginning $\sim$12:30 UT on April 22. This impulsive event extended up to $\gtrsim 1$ MeV in electrons (with $\gtrsim 25$ keV electron fluxes reaching 10^3 $(\mathrm{cm}^2.\mathrm{s.sr})^{-1}$) and $\gtrsim 6$ MeV in protons. There is a complex temporal structure in the electron fluxes at the onset which suggests some spatial channeling of the particles. A second, much weaker, event is detected at WIND beginning $\sim$18:30 UT on April 26 with a much larger increase in >35 keV ions than in >25 keV electrons.

3.3. Optical, radio and X–Ray activity

Optical Hα and K_{IV} observations show an active region #7863 (W 45 S 5 on April 19). The corresponding Yohkoh soft X–Ray region has a similar evolution in time; the activity seems to be maintained even when the region has passed the West limb. The most intense GOES X–Ray burst occurs on April 22, 11:50 UT and corresponds to an intense brightening of the region on the Yohkoh Soft-X–Ray Telescope daily images (Tsuneta et al., 1991).

URAP's RAR spectra for the April 20–30 period show an increasing solar activity starting around April 22. This activity consists of discrete type III bursts and also type III–noise storms (from April 22–26). Some of the type III bursts have been followed from 1 MHz down to some tens of kHz (see Table 2 for their onset times at 1 MHz) and will be later referred to as LFTIII.

During this period (April 20–30) HI-SCALE's X–Ray channels also reveal an increased solar activity in X–Ray bursts. Most of these X–Ray bursts are temporally associated with type III onsets detected by URAP. The first LFTIII during this period occurs on April 22 around 11:50 UT and is associated with a very intense X–ray burst at 11:50 UT observed in the HI-SCALE X–Ray channels. This burst is complex and is composed of successive bursts detected between 11:55 and 12:28 UT. The next LFTIII of this period occurs on April 25, 04:50 UT, and is associated with a soft X–Ray burst beginning at 05:00 UT. These two LFTIII on April 22 and 25 are also observed by WIND. Region#7863 was the only one on the solar disk seen from Earth up to April 22 when it passed behind the limb and was responsible for all the solar activity during this period. It is reasonable to assume that the type III burst observed by URAP is also associated with this region, as well as April 22 events. The fact that no counterpart in radio emission is observed either by Earth Spectrographs (Solar Geophysical Data) or by NRH for this second burst also implies that the active region responsible for the emission observed by Ulysses is on the invisible side of the Sun as seen from Earth.

Solar radio activity observed by the NRH also originates from the same region. The noise storm activity begins on April 20 at 327 MHz. On April 21, a noise storm onset is observed around 12:00 UT at 327 MHz and later on (around 13:45 UT) at 164 MHz. On April 22, the radioheliograph observed an event starting at 11:48 UT. The first outburst is observed at 164 MHz, referred to as #1 on Fig. 4. This burst includes type III bursts and is associated with the onset of a type II burst observed at decameter wavelengths. This event is followed by a bursty continuum enhancement visible at all frequencies, decreasing progressively after 12:30 UT until about 14:00 UT. The positioning of the continuum source in the five observing frequencies is shown in Fig. 4 and illustrates a displacement in position with increasing frequency. The structure implied in this emission is rather radial. In addition, a succession of bursts whose positions are referred to by numbers in Fig. 4, are observed between 11:50 UT and 12:35 UT:

2. corresponds to type III bursts observed at 11:50 and 11:53 UT.
3. is observed only at 164 MHz at 12:20 UT and is not identified on spectral records. In addition between 11:52 and 12:10 UT, a weak moving source (with a projected velocity of about 200 km/s) was also identified (M).
4. is a type III burst group identified at all frequencies between 12:27 and 12:35 UT.

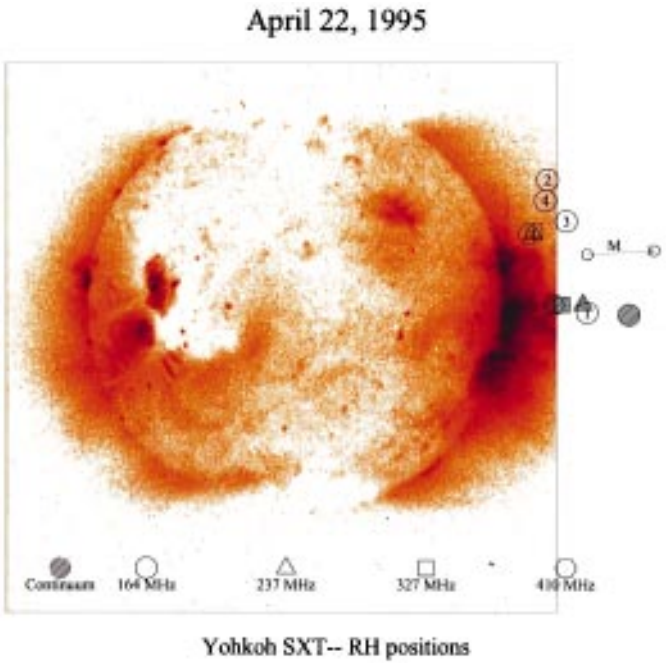

Fig. 4. Yohkoh soft X–ray telescope picture for April 22,1995 09h48m30s UT with superimposed positions obtained with the NRH. The frame around the picture delimits Yohkoh SXT field of view. The positions of the different observing frequencies are labeled as follows: circles for 164 MHz; triangles for 237 MHz; squares for 327 MHz and hexagons for 410 MHz. The different bursts are labeled with numbers 1 for 11:48; 2 for a type III starting at 11:50; 3 burst at 12:20 UT; 4 for the last type III at 12:27. M denotes a moving source between 11:52 and 12:10 UT (displacement is indicated by the arrow) and the shaded areas correspond to the positions of continuum sources. Note that the region implied in this process is close to the arcade system visible on the X–ray picture.

4. Discussion and conclusions

The onset of the gradual electron flux increase observed by WIND up to 300 keV from April 21 to the onset of the April 22 event is in time coincidence with the radio noise storm period observed by the NRH. From joint X–Ray and radio studies (see Lantos et al., 1981 and Crosby et al., 1996), type I noise storm activity has been associated with long–duration electron acceleration. This event is the first direct observational evidence for such a process. The emission site of this activity could be identified by the NRH as active region #7863. When this region rotates behind the West limb of the sun (as seen from Earth) on April 22, it is the location of a major event. The radio coronal signature of this event consists of successive bursts starting at 11:48 UT and originating from distinct regions of the corona, plus, at decameter wavelengths, a type II burst. This shows that the injection of the electron beams responsible for the type III emission is fragmented, not only in time but also in space. The Yohkoh X–ray image reveals a complex arcade system on the western limb, some of which connect the two regions where the radio burst numbers 1 to 4 are produced; others are located near the region where burst numbers 2, 3 and 4 originate (see Fig. 4). This supports the process discussed in Manoharan et al., (1996) implying magnetic reconnection in a complex arcade system is responsible for the acceleration of electrons responsible for the type III bursts. A non–negligible fraction of the particles accelerated during this event, as revealed by the radio continuum, have access to open field lines and the interplanetary medium: they produce the intense impulsive event observed by WIND on April 22 12:00 UT.

Some particles diffuse in the interplanetary magnetic field irregularities to the Ulysses spacecraft where they are detected as the major electron event observed by the spacecraft. The particles here experience a diffusive rather than a direct propagation to Ulysses. This is attested by the essentially isotropic pitch angle distribution and the time delay between the flare and the particle arrival time at Ulysses. As an illustrative example, the propagation of 5.4 MeV protons with a pitch angle of 60° along a path of 1.5 AU takes 4h; this implies that protons injected on April 22, 12:00 UT (flare onset) should reach Ulysses on April 22 around 16:00 UT if they were propagating scatter–free. The transit time of those particles to Ulysses should even be shorter because of adiabatic focusing along the diverging interplanetary magnetic field lines which would rapidly decrease the pitch angle and hence transit time. The 5.4–23 MeV COSPIN/KET proton channel observes the event onset on April 23 around 03:00 UT which is too late compared to April 22 16:00 UT or earlier and implies a non scatter–free propagation. In addition, the extrapolation of the onset time versus the inverse of particle velocity curve is posterior some 4 to 6 hours to the flare time. Such a delay cannot be explained even by non scatter–free propagation. It is therefore likely that the delay in the arrival is also introduced by particle propagation in the solar corona, from the origin site to the exit point at a flux tube connected to the spacecraft. That is, the main source of accelerated particles is the region from which the radio continuum is emitted. The particles accelerated there have access to mid–latitude field lines connected to Ulysses that are opened out to the interplanetary medium by a CME expansion away from the Sun. As the CME expands in the corona, it pushes the overlying field lines and gradually forces them to open on both sides of its structure. If a CME expands at a speed of 300 km/s, it will reach 10 solar radii in some 6.5 h and is only then able to open mid–latitude field lines out to the interplanetary medium. Such a scenario is discussed in Manoharan et al., (1996). If we retain both of these hypotheses (non scatter–free propagation and "corona transit time"), the lack of a low ion energy counterpart (below 500 keV) observed at Ulysses might be due to: a) the very bad connection of the spacecraft, both in latitude and longitude, to the injection site; b) the ionization–loss in the corona (as the particles reaching Ulysses spend more time in the corona than those reaching Earth).

The second event presents no time dispersion between high and low energy proton nor electron channels. It also coincides with the beginning of the 7% flux Forbush–like decrease of the high energy KET channel. The lack of time dispersion could be interpreted as Ulysses' entrance into an interplanetary channel connected to the shock producing the Forbush decrease. As the time profile of the high energy KET channel is not the one usually induced by CIRs (Kunow et al. (1995)), a natural candidate for the shock is the one indicated by the NRH observations on April 22. This shock leaves the solar surface on April 22, 12:00 UT. To reach the Ulysses helioradius by the end of April 25 and therefore shield the spacecraft from cosmic rays, the propagation velocity of this shock should be $\gtrsim$ 870 km/s. This velocity is compatible with commonly–admitted shock front velocities. Plasma experiments aboard Ulysses do not see any clear evidence of the passage of any shock front during this period. But since Ulysses is 37° N and 40° W of the shock originating site (identified by the moving type IV by the NRH above active region#7863), the shock front itself might not be extended enough in latitude and longitude when it reaches the Ulysses helioradius to pass through the spacecraft. As the shock expands away from the sun at helioranges larger than Ulysses, its longitudinal and latitudinal expansion might have grown enough to intercept interplanetary magnetic field lines connected to the spacecraft and therefore shield it from cosmic ray particles. If the region affected by the CME was magnetically connected to field lines running from close to the sun to Earth/WIND, particles accelerated by the shock could then reach Earth as suggested in Reames et al. (1996).

Shock acceleration for the particles measured during the second flux enhancement is also consistent with the Ulysses HI-SCALE measurements of the Ne ions at this time. That is, the source of the Ne ions is interstellar neutral Ne atoms which are ionized by the solar UV fluxes. Rather than being convected to the heliopause for acceleration, some portion of the ionized population is likely to be accelerated by interplanetary shocks and then detected as low energy anomalous cosmic rays (the spectrum of anomalous Ne cosmic rays in the north solar polar region is presented in Lanzerotti et al., this volume). This is probably why Ne ions were detected in this second interplanetary enhancement and not in the first, or in the more than twenty day interval around the entire event.

We must note that an impulsive contribution of solar origin can not be ruled out during this second flux enhancement as might be suggested by the weak electron anisotropy detected by HI-SCALE at its beginning. Ulysses indeed observes a type III burst and its associated X–ray burst around 5:00 UT on April 25. No corresponding radio emission to this type III burst is observed at high frequencies from Earth, implying that the emission site of this burst is on the invisible side of the Sun as seen from Earth. Region #7863 has passed behind the solar limb and is some 40° behind the limb on April 22; and is likely to be the origin of this type III burst, as it was for all previously–observed bursts. The location of region #7863 is much closer to Ulysses' spiral footpoint than it was on the previous days. As the type III and X–ray bursts show, particles were injected into the interplanetary medium. Some of those particles could reach Ulysses' location and contribute to the second electron/ion event described above. Due to the bad connection of Earth to the injection site, particles could diffuse in the interplanetary medium and reach Earth/WIND some 24 hours later than Ulysses. Another possibility is the contribution of these particles to the population that is accelerated by the shock. Impulsive solar injection alone cannot be retained to explain the ion and electron flux histories observed by Ulysses and WIND: the event is much more pronounced in ions than electrons on WIND (see Fig. 3) and is also seen in low energy ion fluxes at Ulysses, a situation which does not seem to favor solar origin particles but rather shock accelerated ones. It is therefore

more likely that those particles are from interplanetary origin: i.e. shock accelerated with possibly a solar contribution.

Acknowledgements. The WIND research at Berkeley is supported in part by NASA grant NAG 5–2815. The research in France is supported by CNRS,CNES and by the Conseil Régional de la région Centre for the NRH operations. We thank the Yohkoh team for providing daily X–Ray data. We would like to warmly thank the referee for the very helpful comments and suggestions he made on this paper.

References

Bame, S. J., McComas, D. J., Barraclough, B. L., et al. 1992, A&AS, 92, 237–265.
Crosby, N., Vilmer, N., et al. 1996, Solar Phys., submitted.
Kunow, H., Dröge, W., Raviart, A., et al. 1995, Proc. 24th Int. Cosmic Ray Conf., Rome, 4, 455–458.
Lantos, P. et al. 1981, A&A, 101, 33–38.
Lanzerotti, L. J. et al. 1992, A&AS, 92, 207.
Lanzerotti, L. J., Maclennan, C. G., Armstrong, T. P., et al. 1996, A&A, this issue.
Lin, R. P., Anderson, K. A., Ashford, S., et al. 1995, Space Sci. Rev., 71, 125–153.
Manoharan, P. K., van Driel-Gesztelyi, L., Pick, M., et al. 1996, Nat, submitted.
Reames, D. V., Barbier, L. M., and Ng, C. K. 1996, ApJ, in press.
Roelof, E. C., Simnett, G. M., Tappin, S. J., et al. 1996, A&A, this issue.
Simpson, J. A. et al. 1992, A&AS, 92, 365–399.
Stone, R. G. et al. 1992, A&AS, 92, 207.
Tsuneta, S. et al. 1991, Solar Phys., 136, 37–67.
The Radioheliograph group. 1993, Adv. Space Res., 13, 9, 411–414.